MODEL BASED PREDICTIVE CONTROL OF AUVS FOR STATION KEEPING IN A SHALLOW WATER WAVE ENVIRONMENT

LCDR Jeffery S. Riedel, USN and Anthony J. Healey
Naval Postgraduate School
Center for AUV Research
Monterey, CA 93943-5000
408.656.1146 voice, 408.656.2238 fax
{jsriedel, healey}@me.nps.navy.mil

Abstract

An important consideration for Autonomous Underwater Vehicles in shallow water is station keeping. Station keeping is the ability of the vehicle to maintain position and orientation with regard to a reference object. In shallow water AUV operations, where large hydrodynamic forces are developed due to waves, knowledge of the sea is critical to allow for the design of a control system that will enable the vehicle to accurately navigate and position itself while in the presence of non-deterministic disturbances.

Recently it has been shown that it is possible to measure the shape of the sea surface using remote sensors such as acoustic probes, lasers or short wavelength radar. These measurements have made it possible to develop so called "predictive" control strategies for many surface applications including hydrofoil operations and craning operations between vessels.

The ability to develop predictive control strategies for underwater vehicles is limited by the ability to measure the environmental disturbances acting on the vehicle. In this paper we describe the design of a model based predictive controller that employs sub-surface sensors for disturbance prediction, to reduce wave induced effects on vehicle station keeping. Using linear wave theory and recursive estimation, an Auto Regressive (AR) model of the sea spectrum is developed. This dynamic model is then used to develop a forward predictor/estimator which is embodied in the controller to cancel the predictable portion of the non-deterministic disturbance on the vehicle thereby minimizing position error. Through simulation the ability of the Naval Postgraduate School's "PHOENIX" AUV to maintain longitudinal position while subjected to actual wave disturbance data from coastal Monterey Bay is shown.

Introduction

For an Autonomous Underwater Vehicle to operate with a high degree of reliability, disturbances and their effects on the AUV must be modeled mathematically with an adequate degree of accuracy. The main source of the dynamic disturbances encountered by underwater vehicles or submerged vessels are wave and current induced. These disturbance forces arise from buoyant and inertial effects due to ocean wave kinematics. The effects of incident waves on a submerged body can be divided up in several categories. The largest, the first order forces act at the incident wave frequency. These forces move the vehicle, but usually result in oscillations about a mean state. Second order forces, which are the result of wave diffraction and wave interaction, have several different frequency components.

Wave diffraction of a single frequency wave results in a steady force and a varying force at twice the wave frequency. The double frequency force may be neglected, as the inertia of the underwater vehicle effectively filters it. Interaction of waves at different frequencies also results in forces. These forces consist of a component acting at the sum of the wave frequencies and a component acting at the difference of the wave frequencies. The force caused by the summation of the wave frequencies, again, may be neglected, as it is also filtered by the vehicle's inertia. The difference frequency component results in a slowly varying force on the AUV. To best assess the performance of a vehicle in shallow water, it is necessary to generate a dynamic model representing the wave induced water velocity and acceleration to properly model the wave disturbance forces.

Since there is strong uncertainty in ocean wave fields, in the past a spectral approach has been best suited for describing the intensity and frequency characteristics of ocean wave fields. During the late 1980's, P. Spanos (1986) presented research on digital simulation of ocean wave disturbances. His research expanded on the use of Linear Prediction Theory (Makhoul, 1975) using Autoregressive (AR) and Autoregressive Moving Average (ARMA) models. Using the former spectral method, considerable numerical difficulties were encountered in getting

Report Documentation Page

Form Approved
OMB No. 0704-0188

1. REPORT DATE	2. REPORT TYPE	3. DATES COVERED
2005		**-**

4. TITLE AND SUBTITLE	5a. CONTRACT NUMBER
MODEL BASED PREDICTIVE CONTROL OF AUVS FOR STATION KEEPING IN ASHALLOW WATER WAVE ENVIRONMENT	5b. GRANT NUMBER
	5c. PROGRAM ELEMENT NUMBER
6. AUTHOR(S)	5d. PROJECT NUMBER
	5e. TASK NUMBER
	5f. WORK UNIT NUMBER
7. PERFORMING ORGANIZATION NAME(S) AND ADDRESS(ES) **Naval Postgraduate School,Center for AUV Research,Monterey,CA,93943-5000**	8. PERFORMING ORGANIZATION REPORT NUMBER
9. SPONSORING/MONITORING AGENCY NAME(S) AND ADDRESS(ES)	10. SPONSOR/MONITOR'S ACRONYM(S)
	11. SPONSOR/MONITOR'S REPORT NUMBER(S)

12. DISTRIBUTION/AVAILABILITY STATEMENT
Approved for public release; distribution unlimited

13. SUPPLEMENTARY NOTES

14. ABSTRACT

An important consideration for Autonomous Underwater Vehicles in shallow water is station keeping. Station keeping is the ability of the vehicle to maintain position and orientation with regard to a reference object. In shallow water AUV operations, where large hydrodynamic forces are developed due to waves, knowledge of the sea is critical to allow for the design of a control system that will enable the vehicle to accurately navigate and position itself while in the presence of non-deterministic disturbances. Recently it has been shown that it is possible to measure the shape of the sea surface using remote sensors such as acoustic probes, lasers or short wavelength radar. These measurements have made it possible to develop so called "predictive" control strategies for many surface applications including hydrofoil operations and craning operations between vessels. The ability to develop predictive control strategies for underwater vehicles is limited by the ability to measure the environmental disturbances acting on the vehicle. In this paper we describe the design of a model based predictive controller that employs sub-surface sensors for disturbance prediction, to reduce wave induced effects on vehicle station keeping. Using linear wave theory and recursive estimation, an Auto Regressive (AR) model of the sea spectrum is developed. This dynamic model is then used to develop a forward predictor/estimator which is embodied in the controller to cancel the predictable portion of the non-deterministic disturbance on the vehicle thereby minimizing position error. Through simulation the ability of the Naval Postgraduate School's "PHOENIX" AUV to maintain longitudinal position while subjected to actual wave disturbance data from coastal Monterey Bay is shown.

15. SUBJECT TERMS

16. SECURITY CLASSIFICATION OF:			17. LIMITATION OF ABSTRACT	18. NUMBER OF PAGES	19a. NAME OF RESPONSIBLE PERSON
a. REPORT	b. ABSTRACT	c. THIS PAGE			
unclassified	**unclassified**	**unclassified**		**26**	

realistic simulations, while the latter methods experienced difficulties accurately approximating a given spectrum, and an accurate approximation could only be feasible when using a high order AR scheme.

In this paper, seaway dynamics will be modeled as a linear Auto Regressive system subjected to random white noise input, where the linear system transfer function is approximately mapped to the local spectrum. Using an LQE approach a predictor, developed from the AR model, is used to predict wave states at future times based on present measurements. Finally, this paper will develop a control scheme to make use of the disturbance estimation and show that station keeping, in the longitudinal (surge) direction, relative to an object, in the presence of shallow water waves is possible.

Linear Wave Theory with Applications to Shallow water

The simplest free surface wave formation, which nevertheless has great practical significance, is the plane progressive wave system. This motion is two dimensional, sinusoidal in time with angular frequency ω, and propagates with a phase velocity c_p such that to an observer moving with this speed the wave appears to be stationary. A cartesian coordinate system is adopted, see Figure 1, with $z = 0$ the plane of the undisturbed free surface (still water level) and the z-axis positive upwards. The vertical elevation of any point on the free surface may be defined by a function $z = \eta(x,t)$. With these requirements, the free surface elevation must be of the general form

$$\eta(x,t) = A\cos(kx - \omega t), \tag{1}$$

where the positive x-axis is chosen to coincide with the direction of wave propagation. Here A is the wave amplitude, and the parameter

$$k = \frac{\omega}{c_p}, \tag{2}$$

is the wavenumber, the number of waves per unit distance along the x-axis. Clearly

$$k = \frac{2\pi}{L}, \tag{3}$$

where the wavelength L is the distance between successive points on the wave with the same phase, Figure 1.

The solution of this problem is expressed in terms of a two dimensional velocity potential, which must satisfy Laplace's equation

$$\nabla^2\phi = 0, \tag{4}$$

and appropriate boundary conditions. Furthermore, ϕ must yield the wave elevation (1) from

$$\eta = -\frac{1}{g}\frac{\partial\phi}{\partial t}. \tag{5}$$

Equation (5) is the linearized dynamic boundary condition on the free surface and is an expression of the fact, through Bernoulli's equation, that the pressure on the free surface must be the same as the ambient atmospheric pressure. An appropriate boundary condition on the sea bottom is

$$\frac{\partial\phi}{\partial z} = 0, \quad \text{at} \quad z = -H, \tag{6}$$

i.e., the bottom at depth H is a rigid impermeable plane. Finally, the free surface boundary condition is

$$\frac{\partial^2 \phi}{\partial t^2} + g\frac{\partial \phi}{\partial z} = 0, \quad \text{on} \quad z = 0. \tag{7}$$

Equation (7) is a combined dynamic and kinematic surface boundary condition. The dynamic condition was discussed earlier, while the kinematic condition simply states,

$$\frac{\partial \eta}{\partial t} = \frac{\partial \phi}{\partial z}, \tag{8}$$

that the vertical velocities of the free surface and fluid particles are the same. Combining (5) and (8), (7) is obtained, ignoring the small departures of the free surface η from the horizontal orientation $z = 0$.

From the requirements of the problem, it is clear that the velocity potential ϕ must be sinusoidal in the same sense as (1); therefore a solution of the form

$$\phi(x, z, t) = \sin(kx - \omega t) F(z), \tag{9}$$

is attempted. Substituting (9) into (4), *F(z)* must satisfy the ordinary differential equation

$$\frac{d^2 F}{dt^2} - k^2 F = 0, \tag{10}$$

throughout the domain of the fluid. The solution to (10) satisfying the bottom boundary condition (6) is

$$F = A\cosh(k(z + H)). \tag{11}$$

Substitution of (9) and (11) into the surface boundary condition (7) yields an important relationship between the wavenumber *k* and the frequency ω,

$$\omega^2 = gk\tanh(kH), \tag{12}$$

which is called the dispersion relationship. The surface elevation η follows from (5)

$$\eta(x, t) = a\cos(kx - \omega t), \tag{13}$$

with the amplitude *a* given by

$$a = \frac{\omega A}{g}\cosh(kH). \tag{14}$$

Substitution of (11) and (14) into the velocity potential function (9) yields

$$\phi(x, z, t) = \frac{ag}{\omega}\frac{\cosh(k(z + H))}{\cosh(kH)}\sin(kx - \omega t). \tag{15}$$

An underlying assumption associated with potential flow theory and Laplace's Equation, is that the velocity field can be expressed as the gradient of a velocity potential function. This allows the expressions for the velocities in the *x* and *z* direction to be given as

$$u = \frac{\partial \phi}{\partial x}$$
$$w = \frac{\partial \phi}{\partial z} \quad . \tag{16}$$

Using (16) and the linearized form of the Bernoulli's equation (17),

$$p = -\rho \frac{\partial \phi}{\partial t} - \rho g z \,, \tag{17}$$

the expressions for the fluid velocity and pressure fields are:

$$u = a\frac{gk}{\omega}\frac{\cosh(k(z+H))}{\cosh(kH)}\cos(kx-\omega t)$$
$$w = a\frac{gk}{\omega}\frac{\sinh(k(z+H))}{\cosh(kH)}\sin(kx-\omega t) \quad . \tag{18}$$
$$p = \rho g a\frac{\cosh(k(z+H))}{\cosh(kH)}\cos(kx-\omega t) - \rho g z$$

It can be seen from (18) that the trajectories of the fluid particles are elliptical.

There are several simplifications that may be made to the above-derived expressions for the cases of shallow (long) and deep (short) water. The shallow and deep water ranges correspond to $H/L < \pi/10$ and $H/L > \pi$ respectively, and over these ranges approximate expressions may be substituted for the hyperbolic functions that have been encountered. Table 1 summarizes these results. Figure 2 depicts the water particle velocity between long and short waves. The key points that should be observed are that shallow water waves are non-dispersive and that the classification of shallow water depends on the ratio of water depth to wavelength.

Table 1. Summary of progressive, small amplitude wave equations

	Deep water (short) waves, $H/L>1/2$, $kH>\pi$	Intermediate depth waves, $1/20 \le H/L \le 1/2$, $\pi/10 < kH < \pi$	Shallow water (long) waves, $H/L < 1/20$, $kH < \pi/10$
In all cases, $\theta=kx-\omega t$			
Profile, η	$\eta = A\cos\theta$	$\eta = A\cos\theta$	$\eta = A\cos\theta$
wave velocity, C	$C = \frac{g}{\omega}$	$C = \frac{g}{\omega}\tanh(kH)$	$C = \sqrt{gH}$
Wavelength, L	$L = \frac{gT^2}{2\pi}$	$L = \frac{gT^2}{2\pi}\tanh(\frac{2\pi H}{L})$	$L = T\sqrt{gH}$
Velocity potential, ϕ	$\phi = \frac{A\omega}{k}e^{kz}\sin\theta$	$\phi = \frac{A\omega}{k}\frac{\cosh(k(z+H))}{\cosh(kH)}\sin\theta$	$\phi = \frac{AgT}{2\pi}\sin\theta$
Particle velocity, u	$u = A\omega e^{kz}\cos\theta$	$u = A\omega\frac{\cosh(k(z+H))}{\cosh(kH)}\cos\theta$	$u = \frac{A\omega}{kH}\cos\theta$
Particle velocity, w	$w = -A\omega e^{kz}\sin\theta$	$w = A\omega\frac{\sinh(k(z+H))}{\cosh(kH)}\sin\theta$	$w = -A\omega(1+\frac{z}{H})\sin\theta$
Pressure, P	$p = \rho g(\eta e^{kz} - z)$	$p = \rho g(\eta\frac{\cosh(k(z+H))}{\cosh(kH)} - z)$	$p = \rho g(\eta - z)$

As an example, consider a one-meter high, monochromatic wave with a ten-second period (0.1 Hz), propagating in water six meters deep. The deep water and shallow water wavelengths are 156 meters and 76.7 meters, respectively. The ratios of water depth to wavelength are 0.038, for the deep water case, and 0.078, for the shallow water case. Referring to Table 1, it can be seen that neither the deep water nor shallow water simplifications may be used. In fact, the water depth must be reduced to 2.45 meters before the shallow water equations are valid. Conversely, if the water depth remains at 6 meters, then the wave period must become greater than 15.6 seconds or the wave frequency less than 0.064 Hz. This indicates that only low frequency waves typically qualify as shallow water (non-dispersive) waves which becomes an important consideration in the proper modeling of the wave induced disturbances. This is shown graphically in Figure 3.

As a side note, it should be pointed out that the wave height has no bearing in determining whether a wave is classified as long or short. The wave height is significant in order to determine the subsurface water particle velocities, and when the wave breaks. As a rule of thumb, a wave will typically begin to break when the wave amplitude approximately equals the water depth, but this is not by any means exact, since other factors, including wave steepness and bottom topography, influence wave breaking.

The plane progressive wave described so far is a single, discrete wave system, with a prescribed monochromatic component of frequency ω and wavenumber k, moving in the positive x-direction. More general wave motions, which are no longer monochromatic, can be obtained by superimposing plane waves of different k and ω. The elevation of the sea surface $\eta(t)$ can thus be described as the superposition of an infinite number of sinusoids of the form:

$$\eta(t) = \sum_{n=1}^{\infty} a_n \cos(k_n x - \omega_n t + \varphi_n) = \sum_{n=1}^{\infty} \eta_n \ . \tag{19}$$

The equations for the horizontal and vertical velocities, accelerations and the dynamic pressure, respectively, are:

$$u(t) = \sum_{n=1}^{\infty} \left[\frac{\omega_n \cosh k_n (H+z)}{\sinh k_n H} \right] \eta_n \qquad ; \tag{20}$$

$$w(t) = \sum_{n=1}^{\infty} \left[\frac{\omega_n \sinh k_n (H+z)}{\sinh k_n H} \right] \eta_n \qquad ; \tag{21}$$

$$p(t) = \rho g \sum_{n=1}^{\infty} \left[\frac{\omega_n \cosh k_n (H+z)}{\cosh k_n H} \right] \eta_n - \rho g z \quad ; \tag{22}$$

where the parameters in (19)-(22) are identical to those in the monochromatic case.

Wave Modeling Using Recursive Methods

A typical experiment in system identification consists in recording a set of input/output data and fitting a parametric model. In discrete time, the first attempt is to fit a Linear Difference Equation (LDE) model of the form

$$y(t) + a_1 y(t-1) + \ldots + a_n y(t-n) = b_1 u(t-1) + \ldots + b_n u(t-n) + \varepsilon(t) \tag{23}$$

with $t \in Z$ denoting the discrete time index, and $\varepsilon(t)$ an error term, accounting for the fact that the data never matches the model exactly. The problem is to estimate the parameter vector

$$\theta = [a_1, \ldots, a_n, b_1, \ldots, b_n]^T \tag{24}$$

from a set of data. In this section we will present the general procedure to estimate the parameters associated with a discrete linear model.

A way of writing (23) is in regression form as

$$y(t) = \varphi(t-1)^T \theta + e(t) \tag{25}$$

with

$$\varphi(t-1) = \left[-y(t-1),\ldots,-y(t-n),u(t-1),\ldots,u(t-n)\right]^T \tag{26}$$

being a sliding window of input and output data. Now the problem is to determine a technique to compute an estimate of the parameter vector θ on the basis of the data set $Z = \{u(0),\ldots,U(N),y(0),\ldots,y(N)\}$, if it is assumed that *N* data points are collected.

If the problem is cast in a probabilistic framework, a probability density for the data set *Z* given the model θ can be written as

$$P(Z|\theta) = \Pr(e(0),\ldots,e(N)) \tag{27}$$

with $e(t) = y(t) - \varphi^T(t-1)\theta$. If we assume the disturbance term sequence to be gaussian and white, then the density on the right hand side becomes

$$\Pr(e(0),\ldots,e(N)) = \prod_{t=0}^{N} \Pr(e(t)) \tag{28}$$

with

$$\Pr(e) = \frac{1}{2\pi\sigma} e^{-\frac{e^2}{2\sigma^2}}. \tag{29}$$

As a consequence it can be seen that

$$\Pr(Z|\theta) = Ce^{-\frac{1}{2\sigma^2}\sum\left|y(t)-\varphi^T(t-1)\theta\right|^2}. \tag{30}$$

As can be seen, minimizing the summation in the exponential can maximize this probability. So if the estimate of the parameters is defined as the vector that minimizes the probability, as

$$\hat{\theta} = \arg\min_{\theta} \Pr(Z|\theta) \tag{31}$$

then it can be computed as a least squares solution

$$\hat{\theta} = \arg\min_{\theta} \sum_{t=1}^{M} \left|y(t) - \varphi^T(t)\theta\right|^2. \tag{32}$$

The solution can be obtained using standard techniques, by writing $\hat{\theta}$ as the least squares solution of the system of equations

$$\begin{bmatrix} y(1) \\ y(2) \\ \vdots \\ y(M) \end{bmatrix} = \begin{bmatrix} \varphi(1)^T \\ \varphi(2)^T \\ \vdots \\ \varphi(M)^T \end{bmatrix} \theta \tag{33}$$

or, compactly

$$y = \Phi\theta \,. \tag{34}$$

The solution given by the pseudoinverse becomes

$$\hat{\theta} = (\Phi^T \Phi)^{-1} \Phi^T y \tag{35}$$

which can be written as

$$\hat{\theta} = \left[\frac{1}{M} \sum_{t=1}^{M} \varphi(t) \varphi(t)^T \right]^{-1} \left[\frac{1}{M} \sum_{t=1}^{M} \varphi(t) y(t) \right]. \tag{36}$$

This is true provided the error sequence $e(t)$ is white and gaussian. If the error is not white, then the estimate of the parameter vector θ is biased.

Now that we have set the foundation, the problem that arises is how do we estimate the parameters associated with a transfer function that will properly represent a model of the seaway in a recursive fashion. If $\hat{\theta}(t)$ is the estimate of the parameters at time *t*, the goal is to compute the successive estimate $\hat{\theta}(t+1)$ by updating $\hat{\theta}(t)$ using the latest observations. It turns out that this problem can be put in a very nice framework that makes use of the considerations on the Kalman Filter.

The AR model, with numerator equal to one, can be written as

$$y(t) = \varphi(t-1)^T \theta + e(t) \tag{37}$$

with *e(t)* a white noise sequence. If it is assume that θ is constant, (37) can be written in state space form, where the state is the parameter vector itself, as

$$\begin{aligned} \theta(t+1) &= \theta(t) \\ y(t) &= \varphi(t-1)^T \theta(t) + e(t) \end{aligned} \,. \tag{38}$$

This is just a particular case of the stochastic state space model with **A** being the identity matrix, **B**=**0** and **C**=$\varphi(t)^T$. This calls for a Kalman Filter approach for the estimation of $\theta(t)$, which leads to

$$\begin{aligned} \hat{\theta}(t+1) &= \hat{\theta}(t) + \frac{\bar{P}(t)\varphi(t-1)}{\lambda^2 + \varphi(t-1)^T \bar{P}(t) \varphi(t-1)} (y(t) - \hat{\theta}(t)^T) \varphi(t-1) \\ \bar{P}(t+1) &= \bar{P}(t) - \frac{\bar{P}(t)\varphi(t-1)\varphi(t-1)^T \bar{P}(t)}{\lambda^2 + \varphi(t-1)^T \bar{P}(t) \varphi(t-1)} \end{aligned} \,, \tag{39}$$

with $\lambda^2 = E\left\{ |e(t)|^2 \right\}$. Clearly this parameter λ is never known, and the need to know it can be eliminated by proper normalization. Dividing the numerator and denominator of (39) by λ^2 the following algorithm is obtained;

$$\hat{\theta}(t+1) = \hat{\theta}(t) + \frac{P(t)\phi(t-1)}{1+\phi(t-1)^T P(t)\phi(t-1)}\left(y(t) - \hat{\theta}(t)^T \phi(t-1)\right)$$
$$P(t+1) = P(t) - \frac{P(t)\phi(t-1)\phi(t-1)^T P(t)}{1+\phi(t-1)^T P(t)\phi(t-1)} \tag{40}$$

which can be easily verified by setting $P(t) = \overline{P}(t)/\lambda^2$. This algorithm is called the Recursive Least Squares (RLS) algorithm.

Using the above developed RLS algorithm the parameters of an Auto Regressive model of the form

$$w(t) + d_1 w(t-1) + \ldots + d_N w(t-N) = e(t), \tag{41}$$

with *w(t)* representing the sea surface elevation due to wave action, and *e(t)*, a zero mean, white noise otherwise know as the innovation, may be developed. The main advantage of the AR model is the fact that the parameter estimation is a linear operation. In fact, if the numerator pertinent to the noise term is not one, then the error state model (38) is not white and we cannot apply Kalman Filtering techniques directly. In the general case, the problem is nonlinear in the parameters and the Extended Kalman Filter must be applied.

The problem that now arises is to determine the order (*N*) of the model to properly reflect the actual frequency spectrum of the time series *w(t)* while keeping the complexity if the model at a minimum. By computing the covariance of the innovation as the order of the model is increased it can be shown that there is a value to which the covariance converges. Using surface wave elevation data obtained in Monterey Bay, from a Waverider measurement buoy, an Auto Regressive model of various orders was determined and the covariance of the innovation compared. The results of this analysis are shown is Figure 4.

As can be seen, the covariance begins to flatten out around an eighth order model. This would have one believe that the correct order model to choose would be an eighth order model. However, as Figure 5 indicates, an eighth order model fails to accurately reflect the actual spectrum. Figures 6 through 8 show that as the order of the model is increased, the error in the matching of the actual spectrum decreases. It is not until a 100^{th} order model that the desired spectrum is actually realized, Figure 9.

There are those that will argue that the energy associated with the low and high frequency modes is minimal, and that proper modeling of those modes is not important. However, as was discussed earlier, it is the low frequency modes of the wave train that are considered shallow water, non-dispersive waves. It is these modes that will have the most effect on the submerged vehicle trying to maintain station. Therefore, as in any design, trade-offs must be made based on analysis, as to how accurate the wave disturbance model must be compared to the resulting controller complexity.

Time Series Transformations Of Surface Wave Records

The simplest method of obtaining information about the wave disturbances in a particular operating area is by surface elevation measurements from a wave buoy. Therefore, it is necessary to be able to transform the wave elevation record into a water particle velocity record at the desired vehicle operating depth in order to determine the proper disturbance model. There are two approaches to this problem. The first uses spectral analysis while the second uses Fourier analysis.

Using the spectral analysis approach, the procedure is to first compute the power spectral density, then use the appropriate modifier and finally convert the spectral density back to time domain. Equation (42) shows this relationship.

$$S_{uu}(\omega) = \left|H(\omega)\right|^2 S_{hh}(\omega) \tag{42}$$

Although the resulting time series reflects the proper magnitude of the water particle velocities, the disadvantage to this method is that all phase information is lost, and the resulting subsurface velocity time series does not reflect the motion caused by the surface elevation times series.

Through the use of Fourier analysis this disadvantage is overcome. In this method, a FFT of the surface wave record is taken, then the Fourier coefficients are multiplied by the appropriate value of the modifier for each frequency component. Once this has been completed, then an inverse FFT is performed. The resulting times series now reflects both the proper amplitude and phase relation.

Figures 10-12 demonstrate this Fourier analysis translation procedure for a wave elevation time series recorded in 30 feet (9.14 m) of water, and translated to a subsurface water velocity record at a depth of 20 feet (6.1 m) in Monterey Bay, CA. It will be this translated velocity record that will be used during the control law design and vehicle simulations later in this paper. The maximum velocity as shown in Figure 12 is approximately 1-knot (0.5144 m/s). It is interesting to note, see Figure 13, that in addition to the dominate peak frequency at 0.12 Hz ,(caused by the wind), there are two additional lower frequency swell generated peaks at 0.05 Hz and 0.07 Hz. Referring back to Figure 4 and Table 1, it can be seen that for this water depth that only the 0.05 Hz frequency component may be treated as a shallow water wave.

AUV Surge Model Development

The equations of motion (EOM) based on constant hydrodynamic coefficients for an underwater vehicle are well known and documented in the literature (Healey, 1993). In general, the hydrodynamic force on a submerged vehicle depends on the relative velocity and acceleration between the water particles and the vehicle. The general case of longitudinal (surge) motion in the *u*-direction written in compact form is

$$(m + X_{\dot{u}})\dot{u}_r + X_{uu}u_r|u_r| = X_{prop}(t) \tag{43}$$

where

$$u_r = (u - U_{fluid}) \tag{44}$$

and $X_{prop}(t)$ represents the propulsion force. The propulsion force can also be modeled in the form

$$\dot{X}_{prop} = \frac{-1}{\mathsf{t}} X_{prop} + \frac{\mathsf{b}}{\mathsf{t}} n|n| \tag{45}$$

where t and b represent a time constant and a thrust parameter, respectively. Combining (43) and (44) and adding the kinematic relations for a vehicle constrained to longitudinal motion, the following system of equations is developed,

$$\begin{aligned} \dot{X} &= u_r + U_{cx} + U_{wx} \\ \dot{u}_r &= \mathsf{a}u_r|u_r| + F_{prop} \\ \dot{F}_{prop} &= \frac{-1}{\mathsf{t}} F + \frac{\mathsf{b}}{\mathsf{t}} n|n| \end{aligned} \quad , \tag{45}$$

where because relative velocities are used in (45), the steady state current and fluctuating velocity caused by waves can be added directly to the kinematic equation. It should be pointed out, that in the form used in (45), *F* becomes a generalized force with unit the same as an acceleration vice a direct thrust value.

With the development of (45) complete, it is desirable to linearize this system of equations about some nominal operating point to simplify the controller design. This nominal operating point can be taken to be a variety of conditions depending on the analysis and control development to be performed. In our case, since we are interested with station keeping, we chose to linearize about the steady state solution to (45) in the presence of a steady current and obtain

$$\begin{aligned} u_{r,0} &= -U_{cx} \\ F_{prop,o} &= \mathsf{a}U_{cx}^2 \\ n_o|n_o| &= \frac{\mathsf{a}U_{cx}^2}{\mathsf{b}} \end{aligned} \quad , \tag{46}$$

as the nominal operating point. Using a standard Taylor series linearization, the linearized system of equations, in state space from, can then be written as

$$\begin{bmatrix} \dot{X} \\ \dot{u}_r \\ \dot{F} \end{bmatrix} = \begin{bmatrix} 0 & 1 & 0 \\ 0 & 2\mathsf{a}\,\mathrm{sgn}(u_0)u_o & 1 \\ 0 & 0 & \dfrac{-1}{\mathsf{t}} \end{bmatrix} \begin{bmatrix} X \\ u_r \\ F \end{bmatrix} + \begin{bmatrix} 0 \\ 0 \\ 2\dfrac{\mathsf{b}}{\mathsf{t}}\mathrm{sgn}(n_o)n_o \end{bmatrix} n + \begin{bmatrix} 1 \\ 0 \\ 0 \end{bmatrix} U_{wx} \quad , \tag{47}$$

$$\vec{\mathrm{y}} = \begin{bmatrix} 1 & 0 & 0 \\ 0 & 1 & 0 \\ 0 & 0 & 1 \end{bmatrix} \begin{bmatrix} X \\ u_r \\ F \end{bmatrix}$$

assuming that all states are measurable. This may be a little pretentious, but it is possible to obtain X and u_r from a doppler sonar with bottom lock, and it would be possible to get thrust measurements directly from the propulsion system if it had strain gauges embedded in the propeller.

If it is assumed that the vehicle will be operating in a 1-knot (0.5144 m) steady current, and the parameters α, β, and τ are available, then equation (47) can be evaluated numerically. As Marco (Marco, 1998) has pointed out, through system identification, it is possible to obtain these values. The values obtained for PHOENIX and reported at IARP '98 are

$$\begin{aligned} \mathsf{a} &= -4.036\ \mathrm{m}^{-1} \\ \mathsf{b} &= 3.962\times 10^{-3}\ \mathrm{m/rev}^2 \\ \mathsf{t} &= 3.14\ \mathrm{s} \end{aligned} \quad . \tag{48}$$

Since the time of Marco's experiments, the PHOENIX has had its propulsion system upgraded, to include larger brushless DC motors for propulsion, increased diameter/pitch propellers and ducted shrouds. From initial at-sea experiments, the vehicle, due to these system upgrades, is now capable of approximately 4-knots (~2 m/s) at 800 revolutions per minute. Based on these upgrades, a more realistic set of values is

$$\begin{aligned} \mathsf{a} &= -4.036\ \mathrm{m}^{-1} \\ \mathsf{b} &= 1.034\ \mathrm{m/rev}^2 \\ \mathsf{t} &= 1.15\ \mathrm{s} \end{aligned} , \tag{49}$$

which will be used throughout the remaining design and simulation.

Since we will be using parameters obtained from a discrete filter, and desire to implement the designed control law into PHOENIX, the state space equations must be converted into a discrete form. Using a standard Euler discretization (47) can be represented in the discrete form as

$$\begin{bmatrix} X(k+1) \\ u_r(k+1) \\ F(k+1) \end{bmatrix} = \begin{bmatrix} 0 & dt & 0 \\ 0 & 1-2\mathsf{a}\,\mathrm{sgn}(u_0)u_o dt & dt \\ 0 & 0 & 1-\dfrac{-1}{\mathsf{t}}dt \end{bmatrix} \begin{bmatrix} X(k) \\ u_r(k) \\ F(k) \end{bmatrix} + \begin{bmatrix} 0 \\ 0 \\ 2\dfrac{\mathsf{b}}{\mathsf{t}}\mathrm{sgn}(n_o)n_o dt \end{bmatrix} n(k) + \begin{bmatrix} dt \\ 0 \\ 0 \end{bmatrix} U_{wx}(k) \quad . \tag{50}$$

$$\bar{\mathrm{y}}(\mathrm{k}) = \begin{bmatrix} 1 & 0 & 0 \\ 0 & 1 & 0 \\ 0 & 0 & 1 \end{bmatrix} \begin{bmatrix} X(k) \\ u_r(k) \\ F(k) \end{bmatrix}$$

Optimal Predictive Controller Development

Using standard optimal control techniques the solution for the optimal (LQR) controller can be found as

$$n = -R^{-1}B^{T}Sx \tag{51}$$

where *S* is found by solving the steady state algebraic Riccati equation (ARE) for the positive definite *S*,

$$A^{T}S + SA - SBR^{-1}B^{T}S + Q = 0\,. \tag{52}$$

Here Q is the weighting matrix on the state error, and R is the scalar, since this is a single input system, that envokes a penalty against the control effort. The LQR approach will always yield a stable system, as long as the Riccati equation provides a positive definite solution matrix *S*.

Figure 14 shows graphically the relation between the level of control input to the level of disturbance rejection for the standard optimal control solution, without a disturbance model included in the control law design. This analysis can give a "feel" for how tight a control law must be provided to achieve a reasonable disturbance rejection. Using the control law design that provides the greatest disturbance rejection, it can be seen in Figures 15 and 16 that a reasonable position is maintained within the propulsion system limitations. To determine how well the propulsion system can respond in the presence of wave induced disturbances, the velocity time series was scaled to a maximum value of 1.5 m/s. At this level of disturbance, the error in maintaining position is +/- 0.4 meters. The required control input, to maintain this position, is greater than the input available from the propulsion system, Figures 17 and 18. If the control law is modified to limit the controller to provide an input within the propulsion system design, then the optimal position control, for this disturbance, is shown in Figures 19 and 20. The problem that now must be solved is how to achieve better performance. We propose, that by embedding a predictor of the disturbance, into the control system design, we can achieve improved station keeping.

The AR model of the wave disturbance may be written in state space form as

$$\begin{aligned} X_{w}(k+1) &= A_{w}X_{w}(k) + B_{w}n(k) \\ y_{w}(k) &= C_{w}X_{w}(k) \end{aligned}, \tag{53}$$

with the only measurement that is available is the wave velocity at current time *k* obtained from the Doppler. If the system is forward time shifted, then information about the future disturbance is available based on current measurements. Equation (54) represents this;

$$w(t+N) + d_{1}w(t+N-1) + \ldots + d_{N}w(t) = e(t)\,. \tag{54}$$

This is possible since the basis of the model is that *e(t)* is white noise. Now by augmenting the vehicle state equations with the disturbance state equations, a new control law may be developed using the predicted disturbance states. To do this a new state vector is defined as

$$X_{aug} = \begin{bmatrix} X_{vehicle} \\ X_{wave} \end{bmatrix}, \tag{55}$$

where the disturbance states are given as

$$X_{w} = \left[X_{w}(k+N-1), \ldots, X_{w}(k+1)\right]^{T}\,, \tag{56}$$

then using the separation principle, the control law is designed assuming all states are measurable. Therefore, as in the previous optimal control discussion, the ARE is solved to obtain the appropriate gains for the augmented system.

This augmented system is

$$X_{aug}(k+1) = \begin{bmatrix} A_{vehicle} & FC_w \\ 0 & A_w \end{bmatrix} X_{aug}(k) + \begin{bmatrix} B_{vehicle} \\ 0 \end{bmatrix} n(k) + \begin{bmatrix} 0 \\ B_w \end{bmatrix} \mathrm{n}(k). \tag{57}$$

With the control law designed the estimator/predictor must be designed. Using optimal estimation theory, a estimator/predictor of the form

$$\hat{X}_w(k+1) = (A_w - LC_w)\hat{X}_w(k) + Lw(k), \tag{58}$$

where *w(k)* is the current disturbance measurement, was developed.

To display how well this procedure can work if an accurate model of the disturbance is available, consider the simple case of a sine wave with only one frequency component as the wave disturbance. The precise model of this disturbance is known. When this model is embedded in the control system design, perfect cancellation of the wave disturbance effects on station keeping may be obtained. These results are displayed in Figures 21 and 22. Now these results are for demonstration purposes only, and we do not expect to get perfect cancellation of the wave disturbances since an exact model of the random sea is not available.

Using the same weighting values that went into the design of the control law that was used in the simulation of the results presented in Figures 19 and 20, improved results are achieved from this method when an eighth order AR model is used to form the predictor, see Figures 23 and 24. As can be seen, there is a 400% improvement in station keeping, and the control input requirements are significantly less. This reduction in control effort is particularly important given the fact that power consumption is the downfall of AUVs.

Conclusions

This paper has shown that an Auto Regressive model provides a convenient means of matching the wave induced disturbance dynamics. It has been concluded that a digital estimator/predictor derived from a low order AR model provides adequate prediction of the disturbances acting on the submerged vehicle. What cannot be concluded from this particular work is the degree of optimality to which the embedded predictor provides, since this analysis was done under ideal conditions, i.e. no noise and all states available. Thus far, based on previous studies in this area, the work conducted herein has indicated a promising direction for improved prediction of wave disturbances on submerged vehicles and the resulting control required to allow the vehicle to maintain station.

The estimator developed is merely a baseline version for predicting the disturbance. That is, since the AR model from which the estimator was developed was assumed to have linear time invariant parameters, the estimator may not accurately reflect the actual dynamics of the disturbance.

Lastly, it should be noted that the optimal predictive control law developed provides excellent disturbance rejection in the presence of wave induced disturbances.

Recommendations

First, it is recommended that further investigations be made into the modeling of wave induced disturbances. The ability to identify the predominate frequency components and use a frequency weighted non-linear RLS algorithm to determine the disturbance model parameters used in the controller design will improve the ability of the vehicle to maneuver and hold station in the presence of wave induced disturbances.

Second, the parameters of the disturbance model should be considered to be time varying, and an adaptive algorithm developed to increase the accuracy of the disturbance model used in the control law design. This parameter identification can be done as a background process, with the resulting parameters passed to the controller.

Lastly, models of vehicle sensor performance in shallow water must be developed to allow for a detailed analysis to determine how and which sensor(s) should be used to measure the wave induced disturbances, and how accurate these measurements will be.

Acknowledgement

The authors wish to thank Dr. Kam NG of the Office of Naval Research for his financial support under contract number N0001496WR20037.

References

Astrom, K.J., and Wittenmark, B., *Adaptive Control*, Addison-Wesley, 1989.

Astrom, K.J., and Wittenmark, B., *Computer Controlled Systems Theory and Design*, Prentice-Hall, 1984.

Bryson, A.E. and Ho, Y.-C., *Applied Optimal Control*, John Wiley & Sons, 1975.

Dean, R.G., and Dalrymple, R.A., *Water Wave Mechanics for Engineers and Scientists*, Prentice-Hall, 1984.

Faltinsen, O.M., *Sea Loads on Ships and Offshore Structures*, Cambridge University Press, 1990.

Friedland, B., *Control System Design*, McGraw-Hill, 1986.

Grimble, M. J., "State-Space Approach to LQG Multivariable Predictive and Feedforward Optimal Control", *Transactions of the ASME*, Vol. 116, Dec. 1994.

Healey, A.J. and Lienard, D., "Multivariable Sliding Mode Control for Autonomous Diving and Steering of Unmanned Underwater Vehicles", *IEEE Journal of Oceanic Engineering*, vol. 18 no. 3, July 1993, pp. 327-339.

Kinsman, B., *Wind waves, their generation and propagation on the ocean surface*, Prentice-Hall, 1965.

Makhoul, J., "Linear Prediction: A Tutorial Review," *Proceedings IEEE*, Vol. 63, Apr. 1975, pp. 561-580.

Marco, D., Martins, A., and Healey, A.J., "Surge Motion Parameter Identification for the NPS Phoenix AUV", to be presented at the First International Workshop on Autonomous Underwater Vehicles for Shallow Waters and Coastal Environments, Lafayette LA, 17-19 February 1998.

Newman, J.N., *Marine Hydrodynamics*, MIT Press, 1977.

Ni, S.Y., Zhang, L., and Dai, Y.S., "Hydrodynamic Forces on a Moving Submerged Body in Waves", *International Shipbuilding Progress*, Vol. 41, pp. 95-111, 1994.

Riedel, J.S., and Healey, A.J., "A Discrete Filter For The Forward Prediction Of Sea Wave Effects On AUV Motions", Proceedings of the Tenth International Symposium on Unmanned Untethered Submersible Technology, Autonomous Undersea Systems Institute, September 7-10, 1997.

Sarpkaya, T. and Isaacson, M., *Mechanics of Wave Forces on Offshore Structures*, Van Nostrand Rienhold Company Inc,, 1981.

Spanos, P-T.D., "ARMA Algorithms for Ocean Wave Modeling," *ASME Journal of Energy Resources Technology*, Vol. 23, No. 1, Mar. 1979, pp. 76-84.

Spanos, P-T.D., and Hansen, J.E., "Linear Prediction Theory for Digital Simulation of Sea Waves," *ASME Journal of Energy Resources Technology*, Vol. 103, No. 1, Sep. 1981, pp. 243-249.

Tolliver, J,V., "Studies on Submarine Control for Periscope Depth Operations", Engineer's Thesis, Naval Postgraduate School, September 1996.

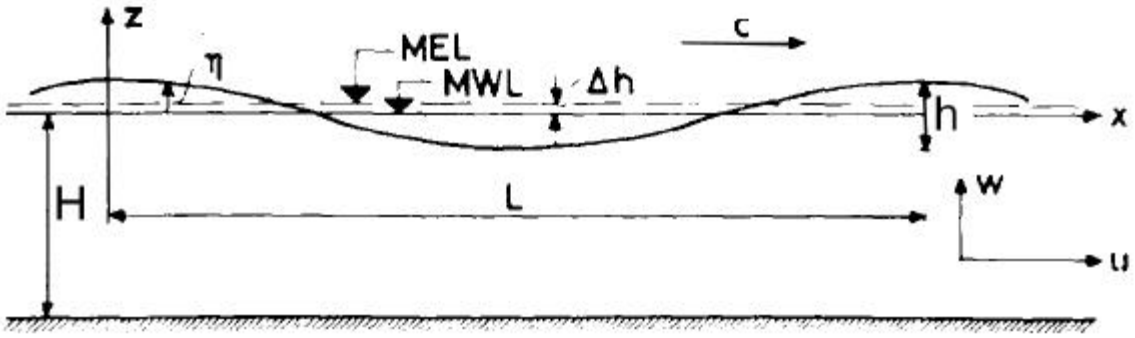

Figure 1. Monochromatic Progressive Surface Gravity Wave

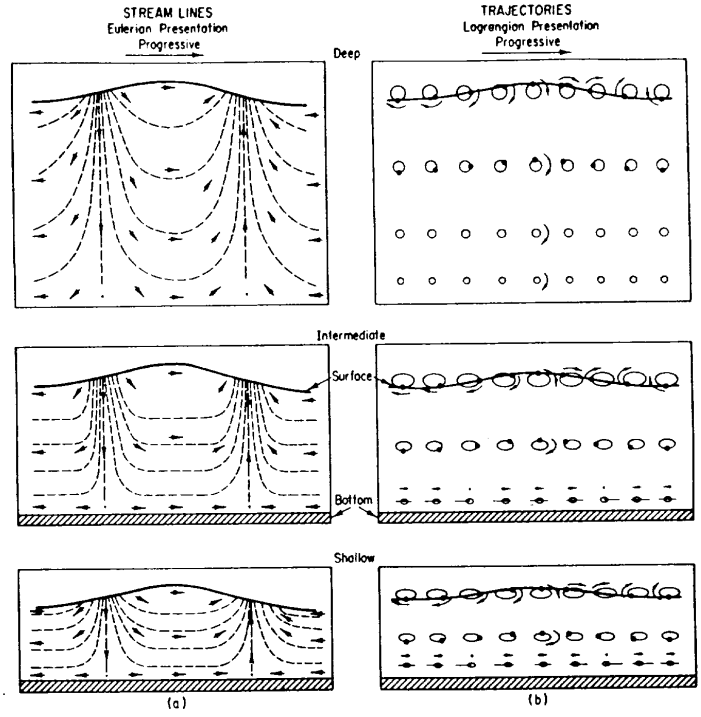

Figure 2. Comparison Of Water Particle Velocities For Different Types Of Waves

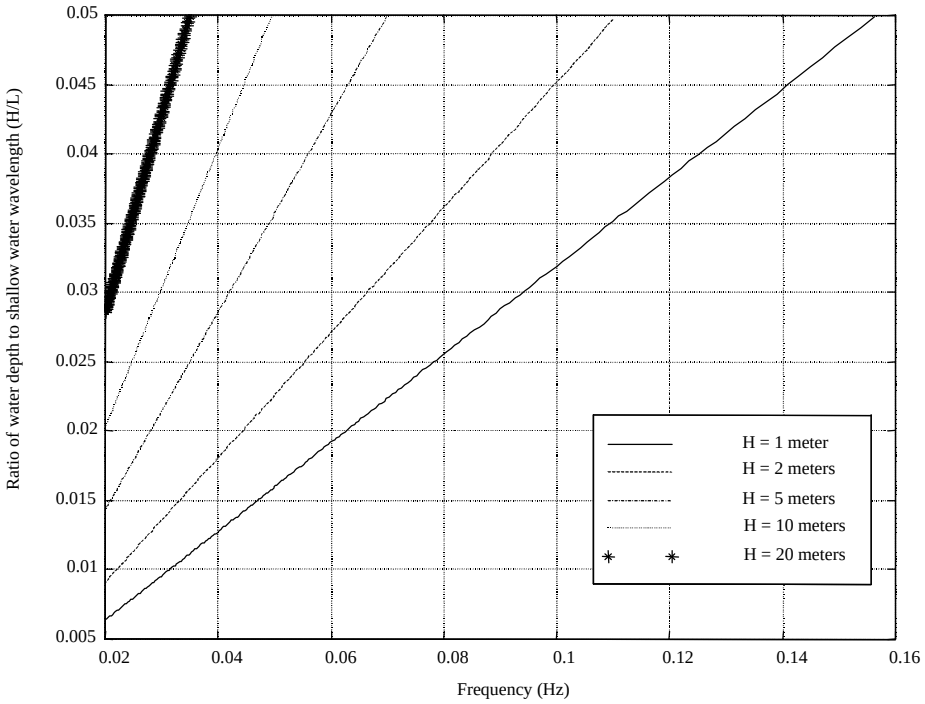

Figure 3. Comparison Of Shallow Water Wavelength Ratio To Wave

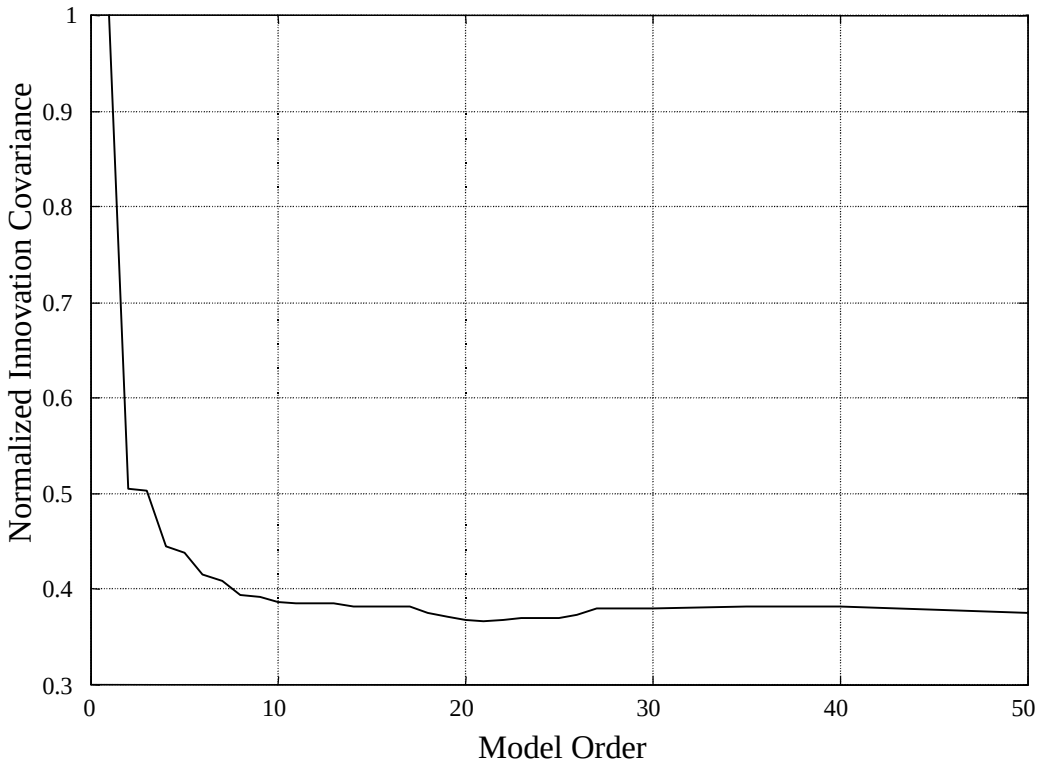

Figure 4. Comparison Of Innovation Covariance To AR Model Order

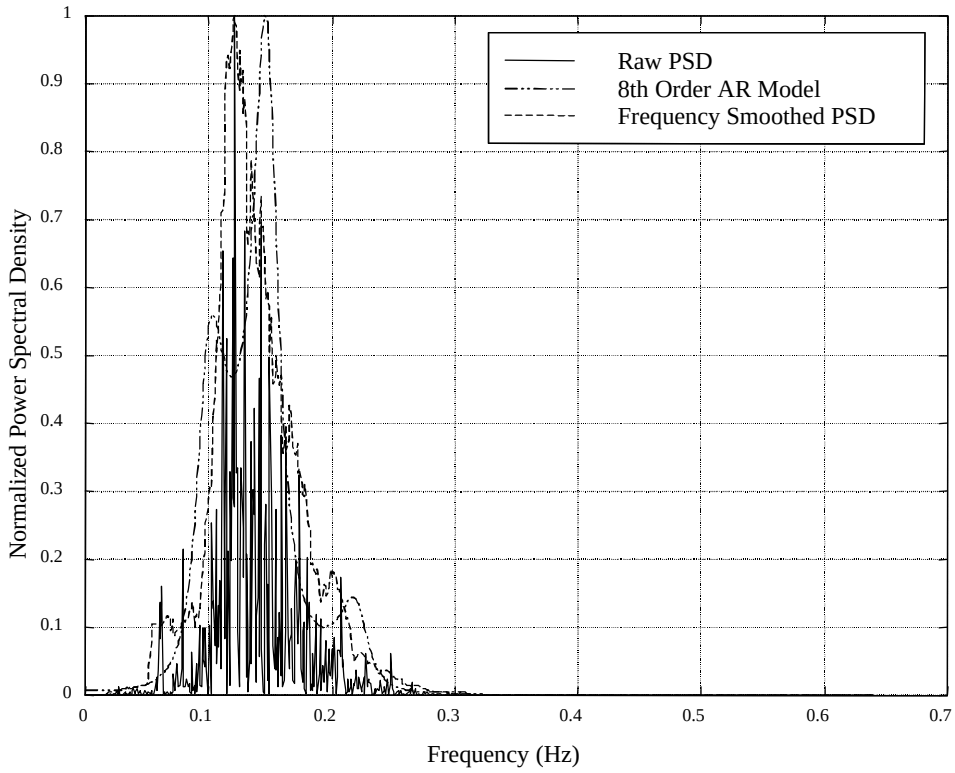

Figure 5. 8th Order AR Model

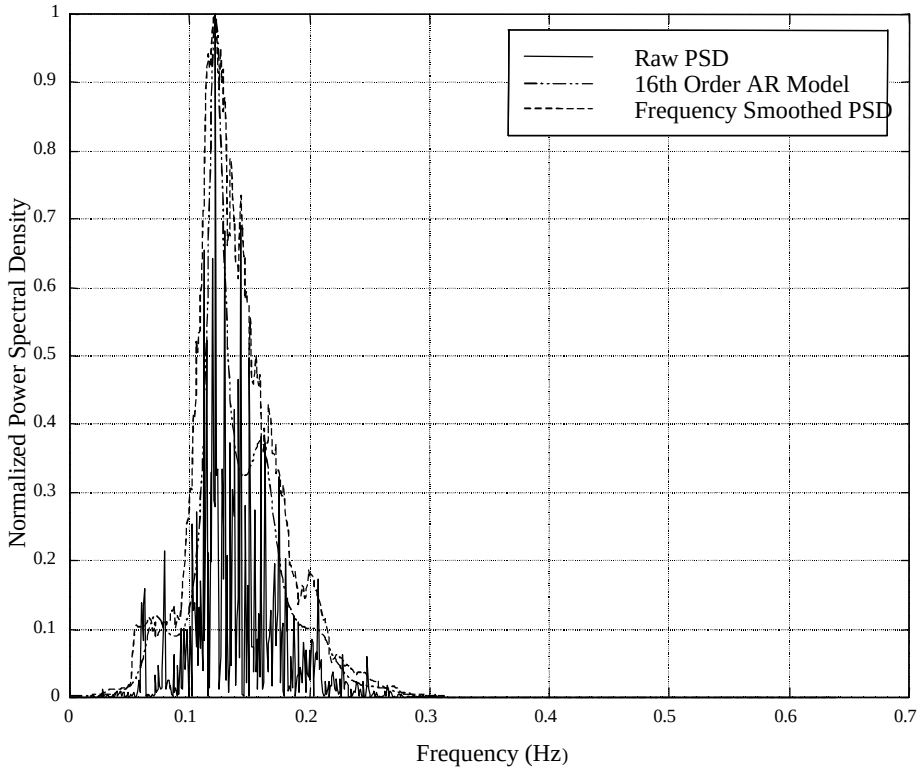

Figure 6. 16th Order AR Model

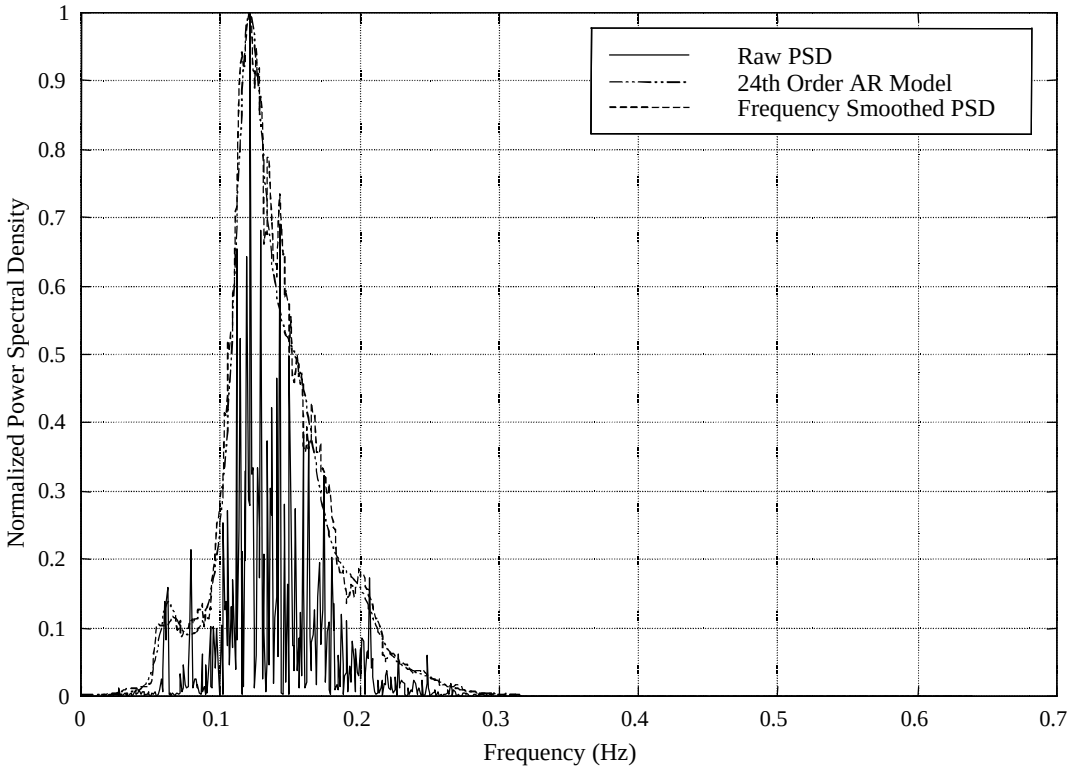

Figure 7. 24th Order AR Model

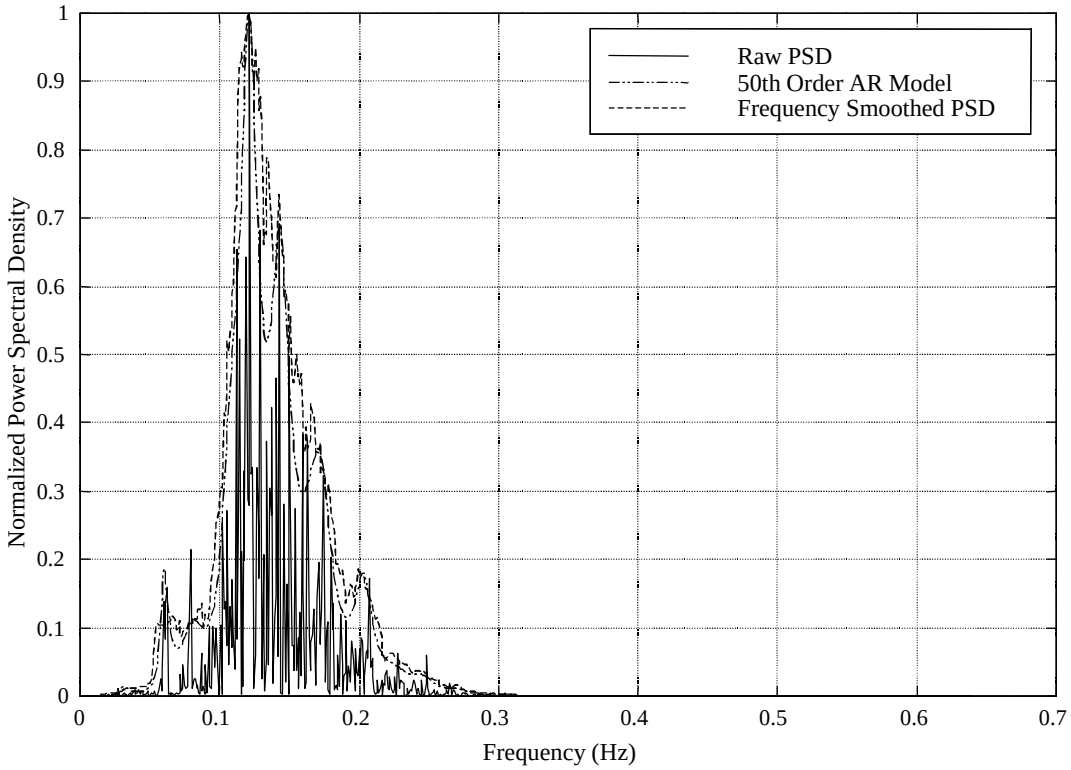

Figure 8. 50th Order AR Model

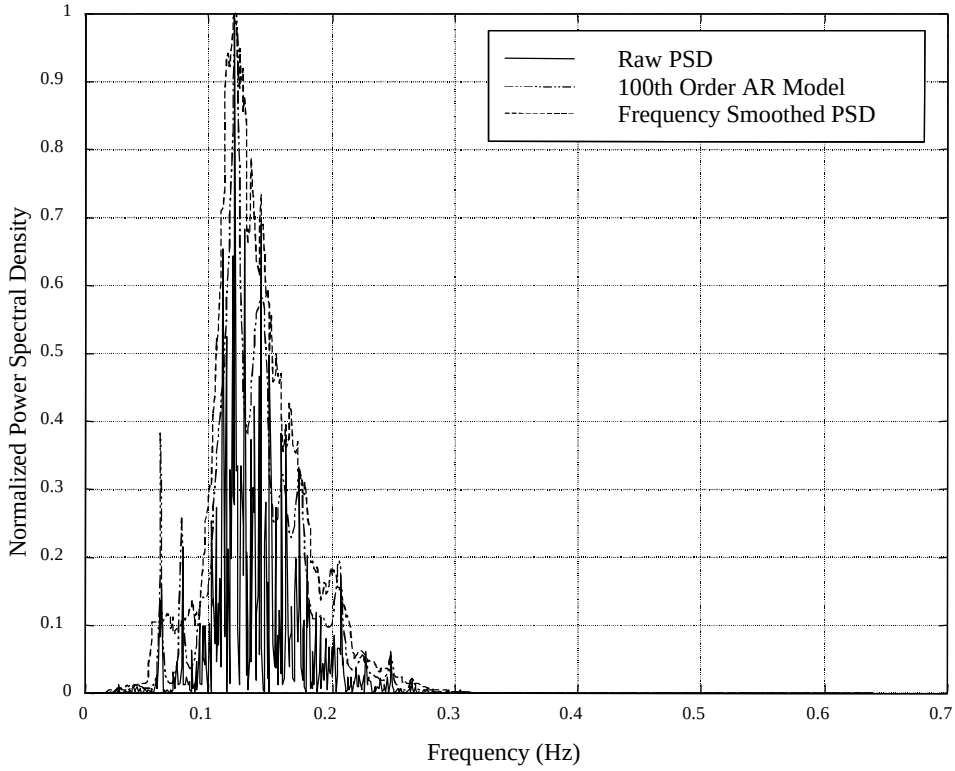

Figure 9. 100th Order AR Model

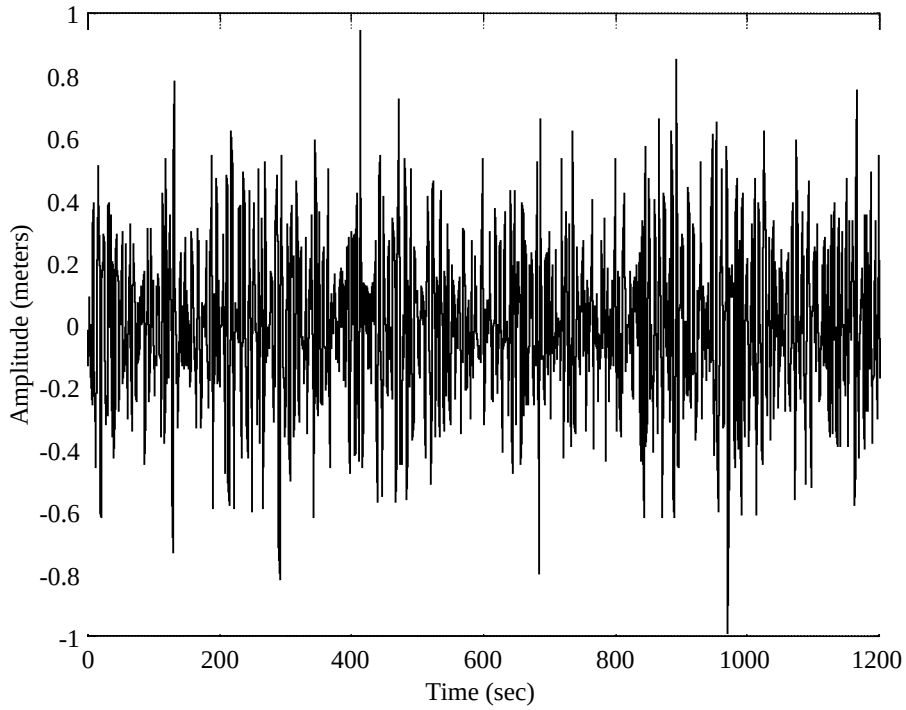

Figure 10. Surface Elevation Time Series

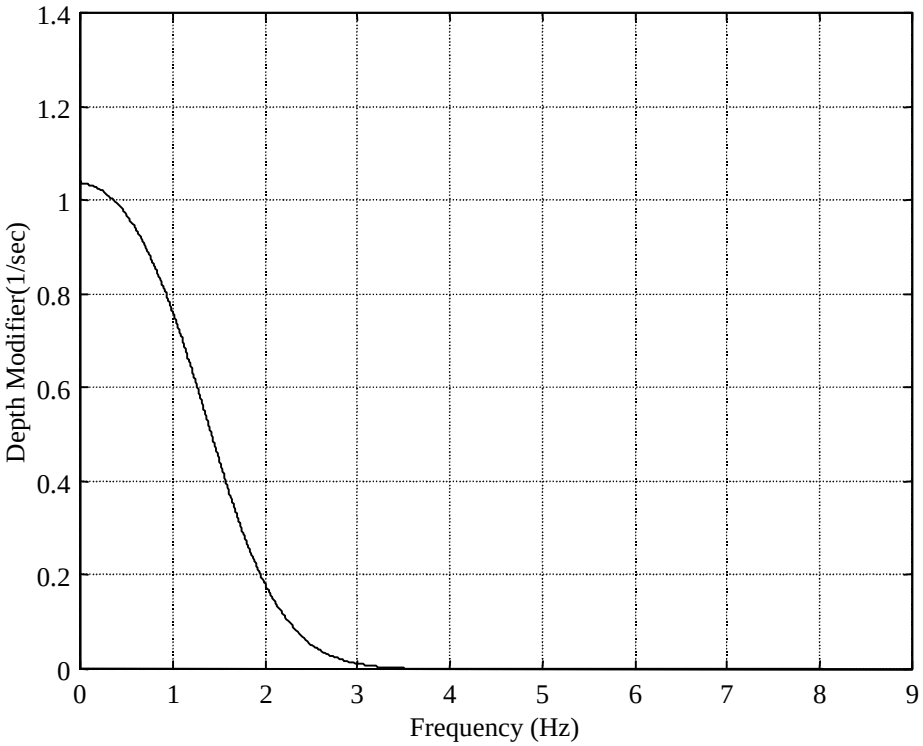

Figure 11. Modifier For Translation Of A Surface Elevation Time Series To A Subsurface Velocity Time Series For A Water Depth Of 9.14 Meters (30 Feet) And An Operating Depth Of 6.1 Meters (20 Feet)

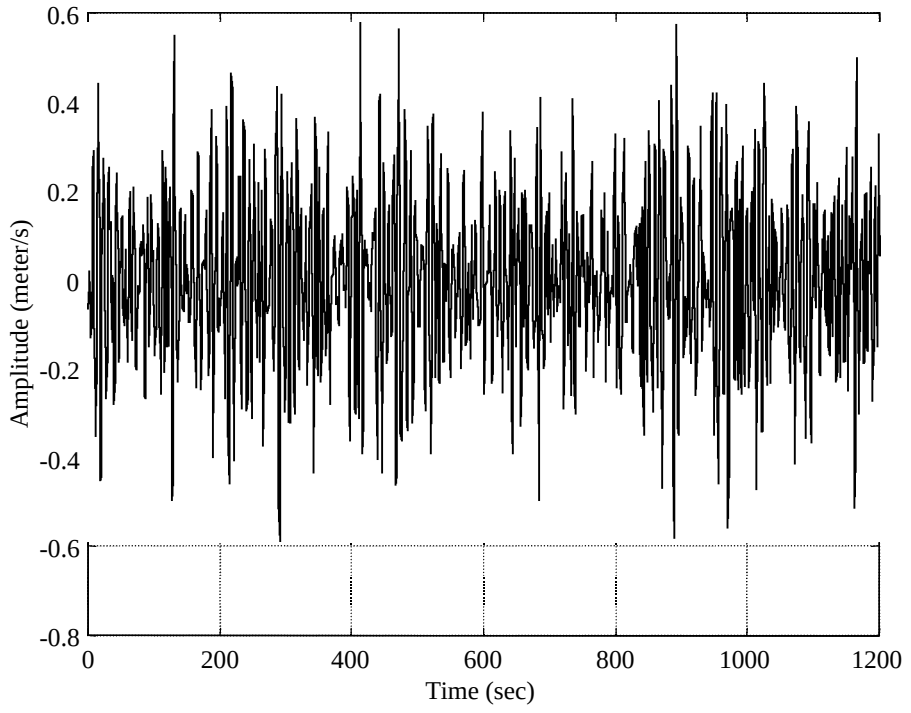

Figure 12. Subsurface Velocity Time Series At Operating Depth Of 6.1 Meters (20 Feet)

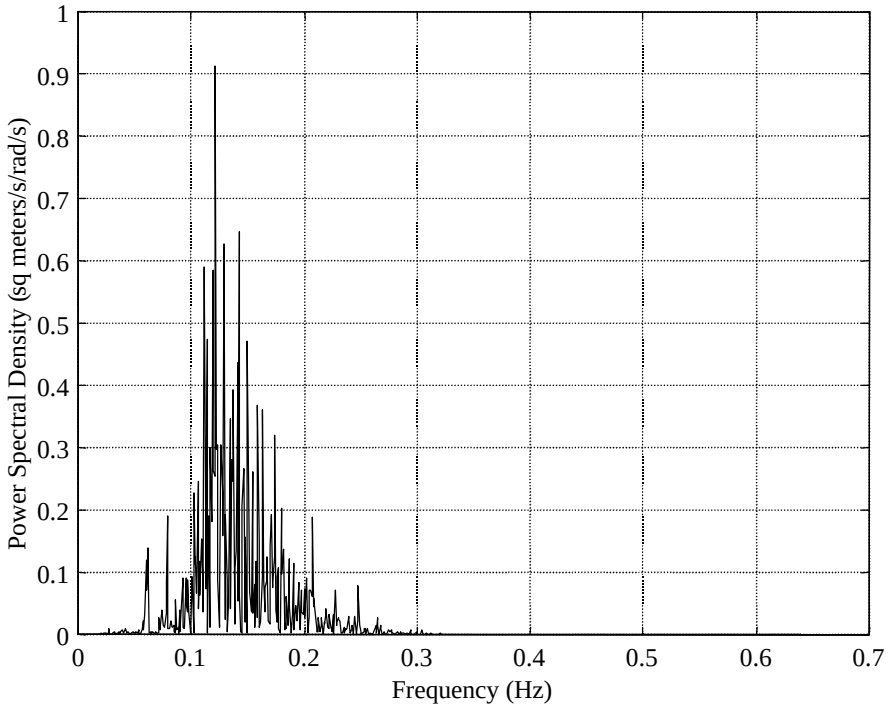

Figure 13. Power Spectral Density Of Subsurface Velocity Record

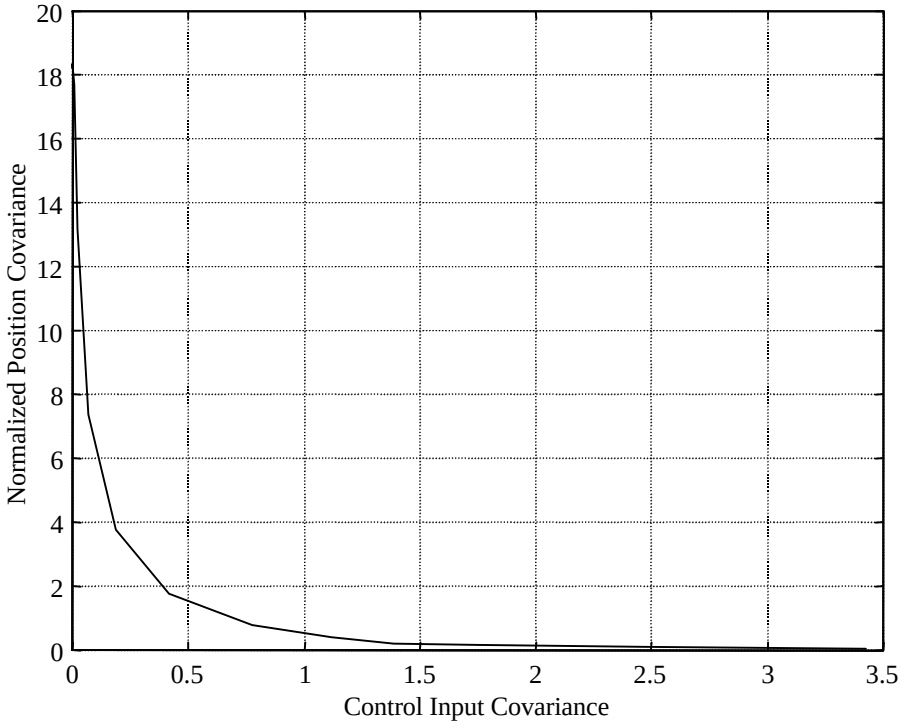

Figure 14. Comparison Of Control Input Covariance To Normalized Vehicle Position Covariance

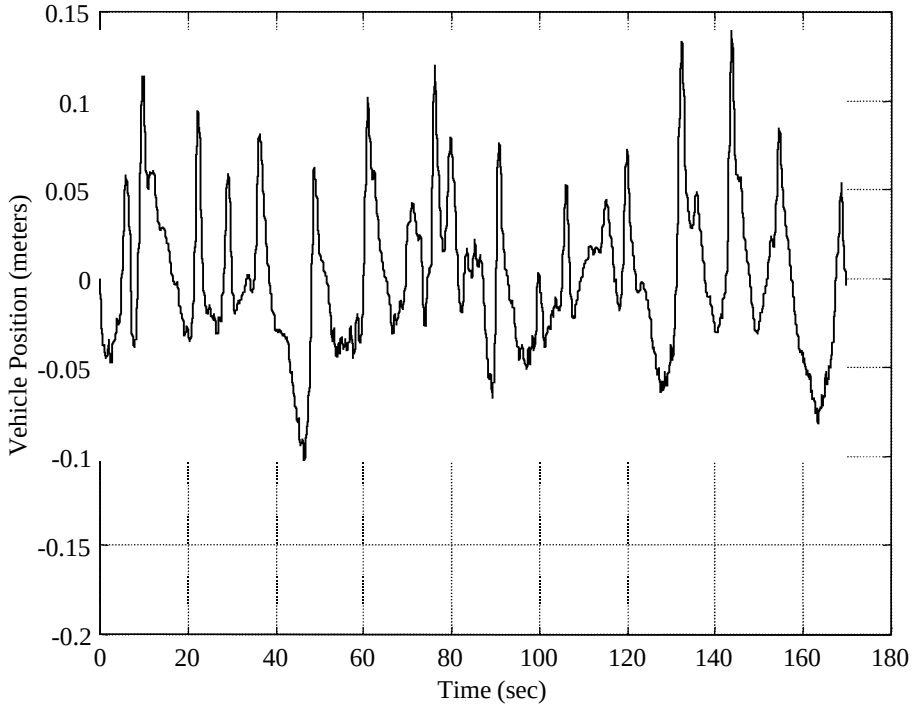

Figure 15. Results Of Vehicle Station Keeping Using Optimal Control Solution In The Presence Of A 1-Kt (0.5144 m/s) Wave Induced Disturbance

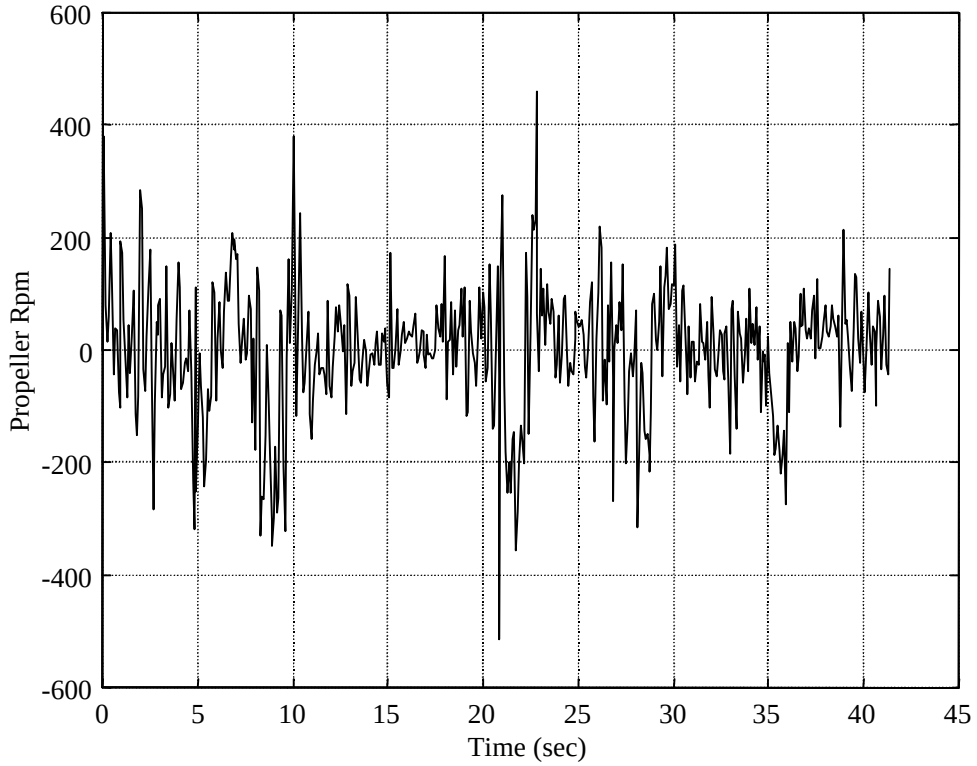

Figure 16. Propeller RPMs From Optimal Control Solution In The Presence Of A 1-Kt (0.5144 m/s) Wave Induced Disturbance

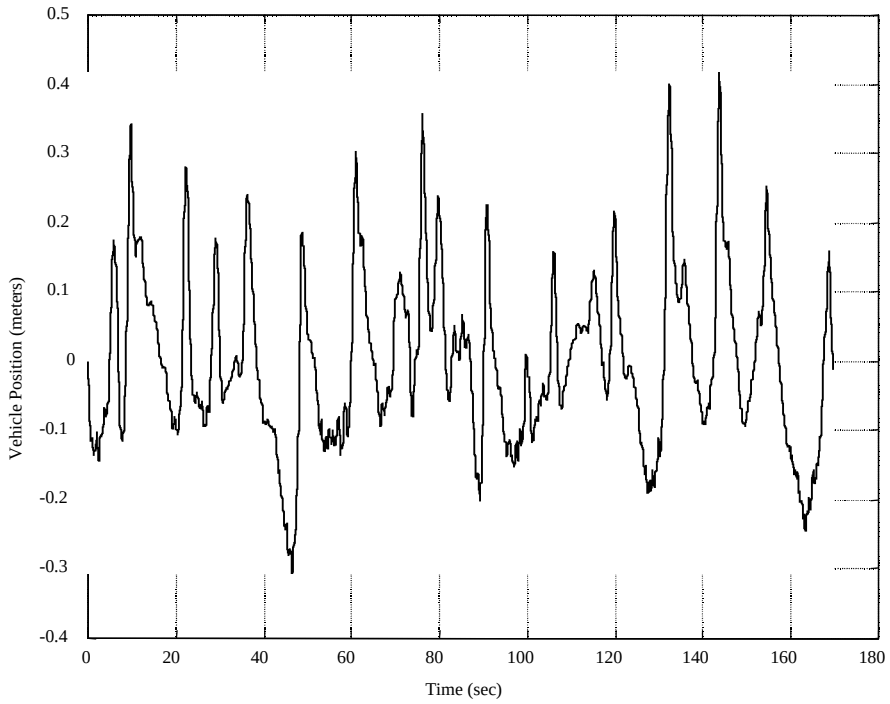

Figure 17. Results Of Vehicle Station Keeping Using Optimal Control Solution In The Presence Of A 3-Kt (1.5 m/s) Wave Induced Disturbance

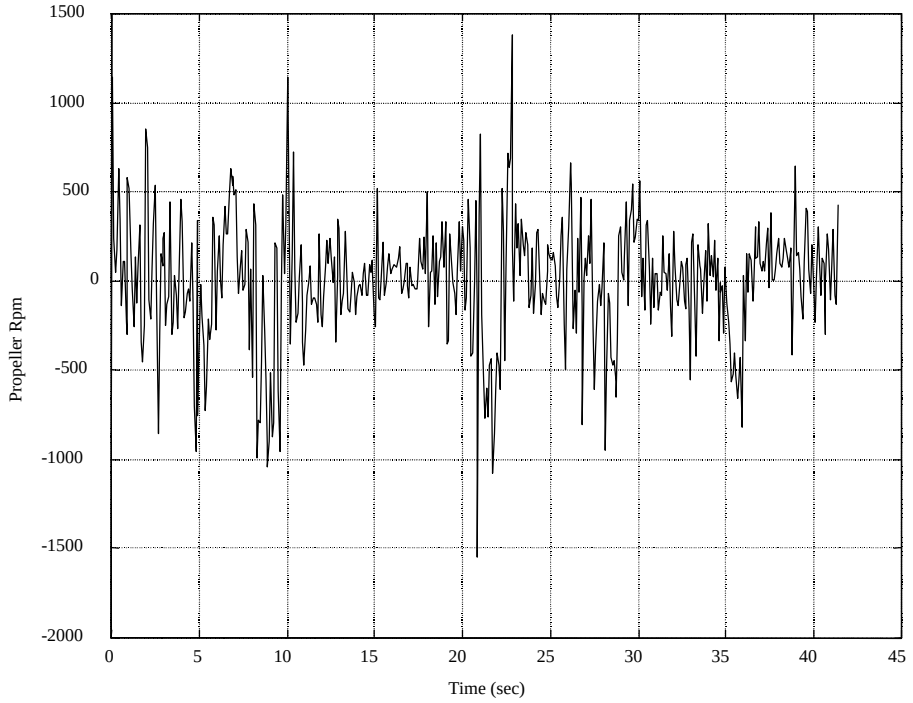

Figure 18. Propeller RPMs From Optimal Control Solution In The Presence Of A 3-Kt (1.5 m/s) Wave Induced Disturbance

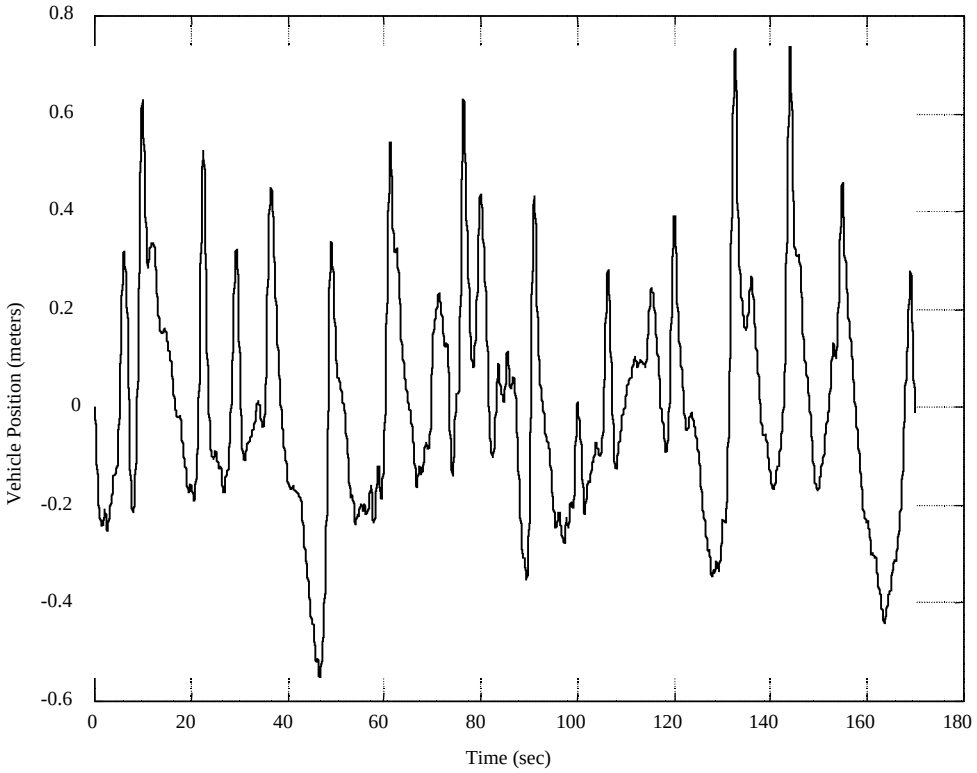

Figure 19. Results Of Vehicle Station Keeping Using Optimal Control Solution In The Presence Of A 3-Kt (1.5 m/s) Wave Induced Disturbance With A Control Input Within Operating Limits

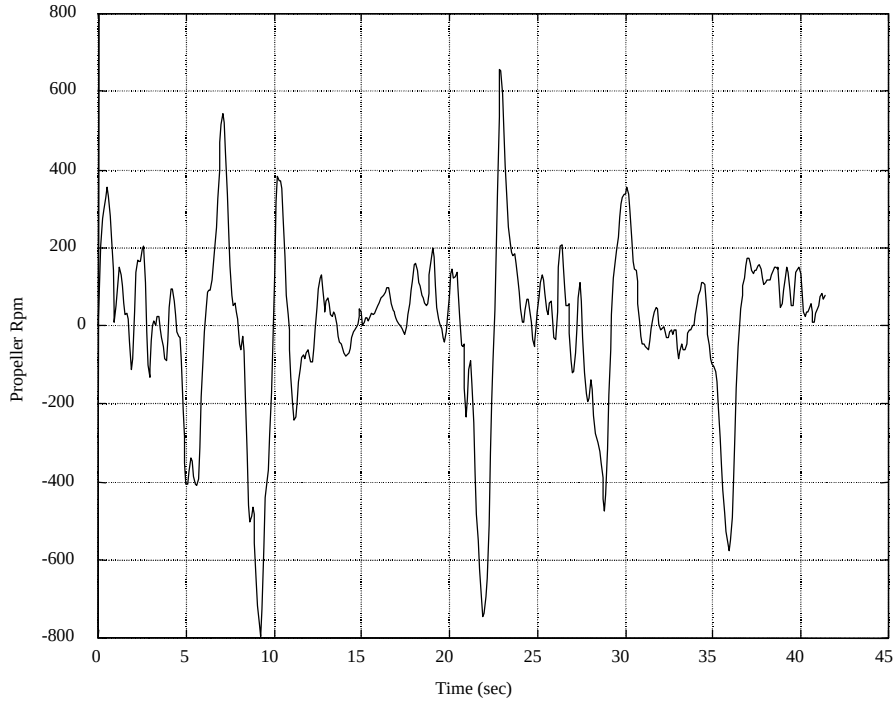

Figure 20. Propeller RPMs From Optimal Control Solution In The Presence Of A 3-Kt (1.5 m/s) Wave Induced Disturbance With A Control Input Within Operating Limits

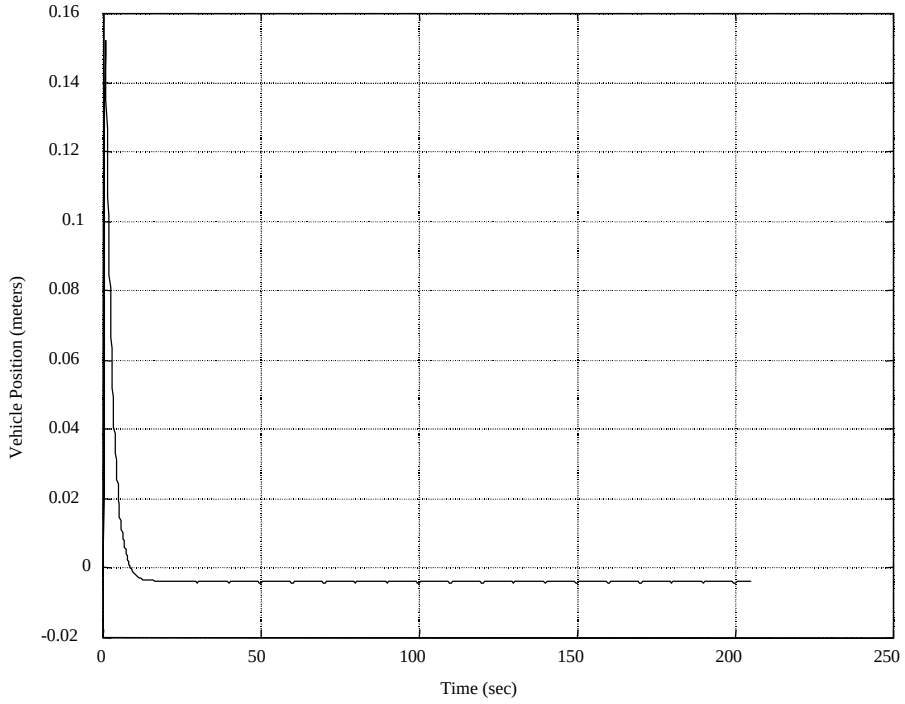

Figure 21. Results Of Vehicle Station Keeping Using Predictive Optimal Control Solution In The Presence Of A 2-Kt (1 m/s) Sine Wave Disturbance

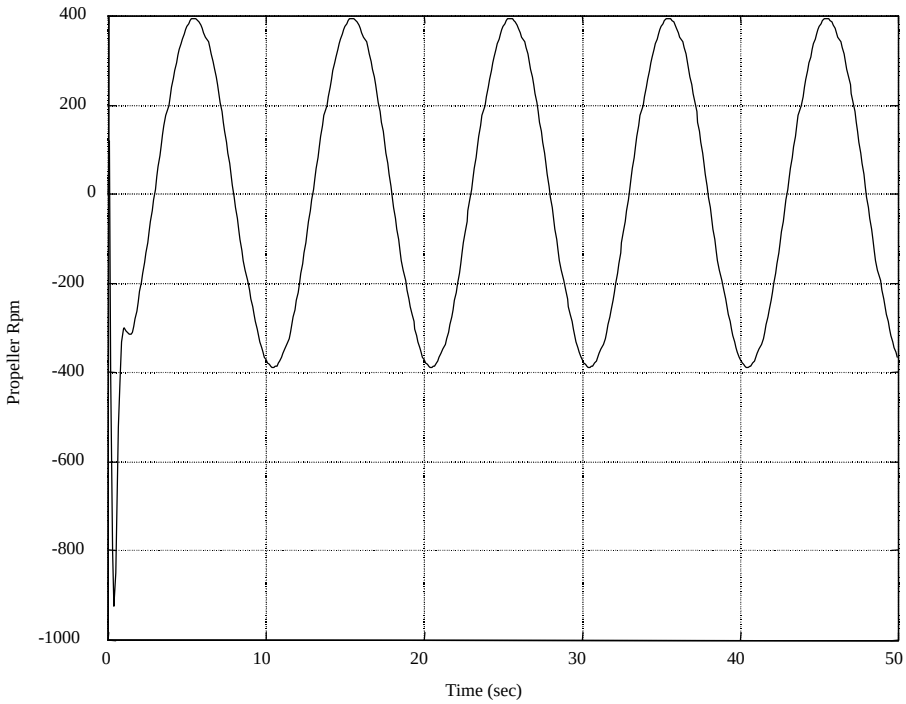

Figure 22. Propeller RPMs From Optimal Predictive Control Solution In The Presence Of A 2-Kt (1 m/s) Sine Wave Disturbance

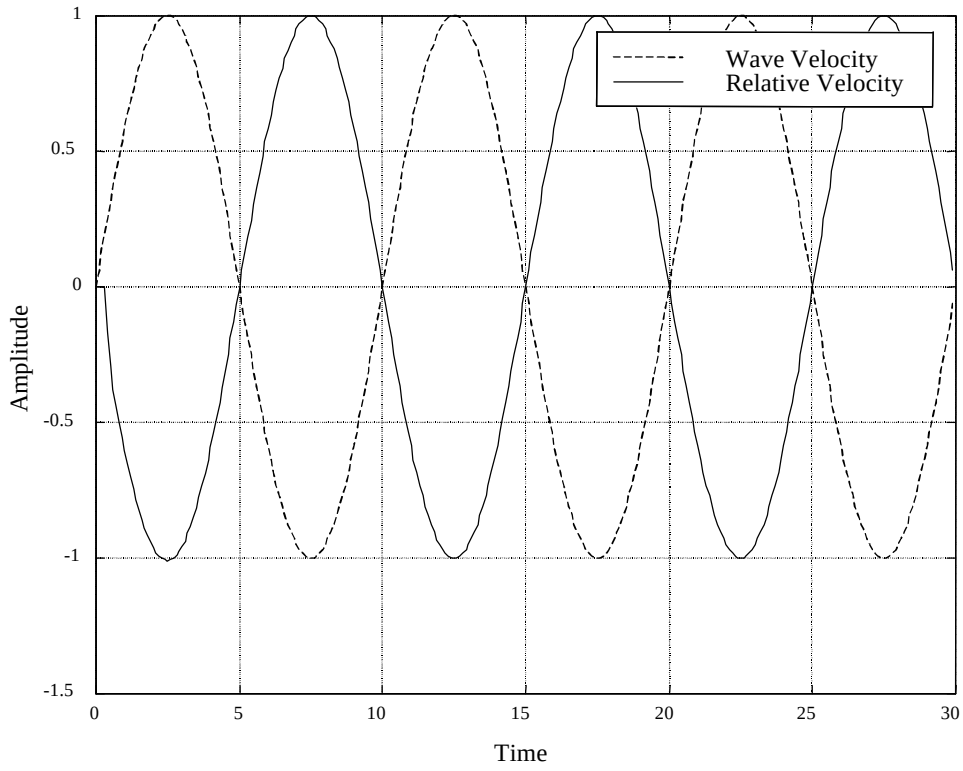

Figure 23. Vehicle Relative Velocity And Wave Induced Velocity vs. Time

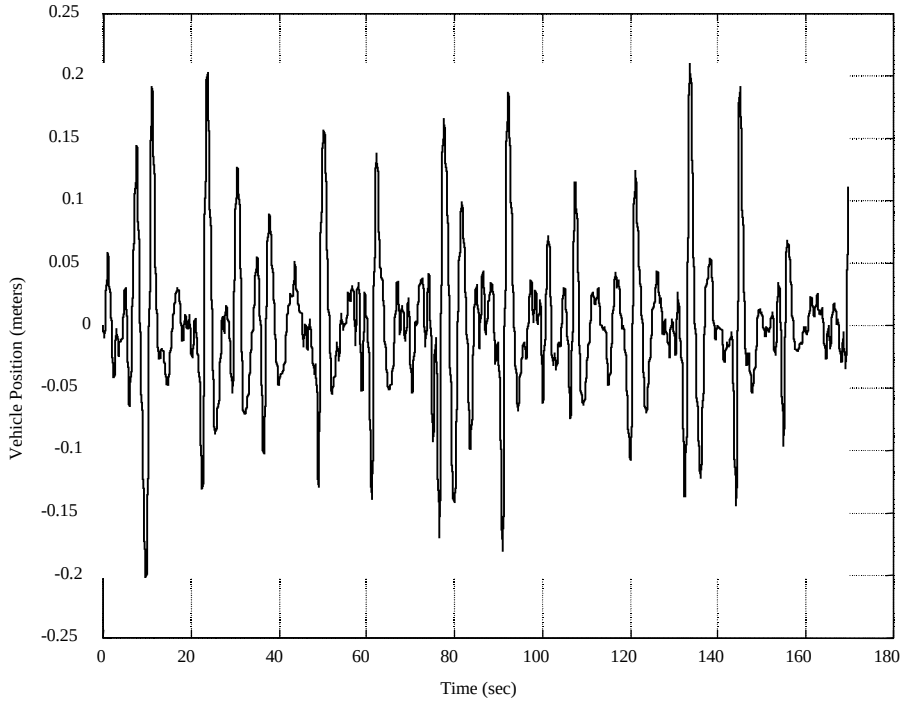

Figure 24. Results Of Vehicle Station Keeping Using Embedded Disturbance Model And Identical Weighting Values As Those Associated With The Results In Figure 19

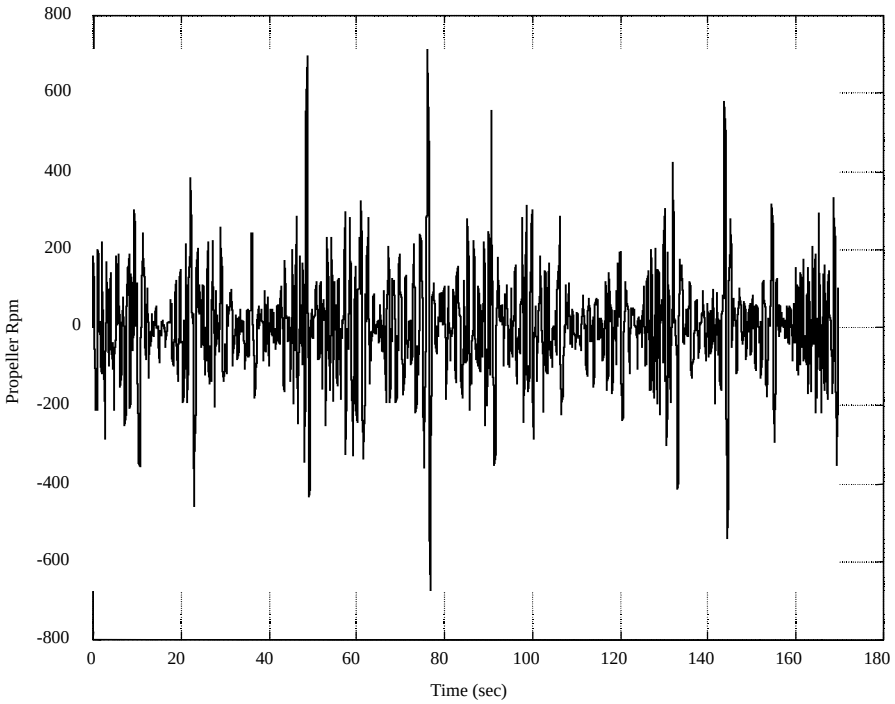

Figure 25. Propeller RPMs From Optimal Predictive Control Solution Using An Embedded Disturbance Model Identical Weighting Values As Those Associated With The Results In Figure 19